Non-Markovian entanglement dynamics of noisy continuous-variable quantum channels

Jun-Hong An[1,2] and Wei-Min Zhang[1,3]

[1]*Department of Physics and Center for Quantum Information Science, National Cheng Kung University, Tainan 70101, Taiwan*
[2]*Department of Modern Physics, Lanzhou University, Lanzhou 730000, People's Republic of China*
[3]*National Center for Theoretical Science, Tainan 70101, Taiwan*

We investigate the entanglement dynamics of continuous-variable quantum channels in terms of an entangled squeezed state of two cavity fields in a general non-Markovian environment. Using the Feynman-Vernon influence functional theory in the coherent-state representation, we derive an exact master equation with time-dependent coefficients reflecting the non-Markovian influence of the environment. The influence of environments with different spectral densities, e.g., Ohmic, sub-Ohmic, and super-Ohmic, is numerically studied. The non-Markovian process shows its remarkable influence on the entanglement dynamics due to the sensitive time dependence of the dissipation and noise functions within the typical time scale of the environment. The Ohmic environment shows a weak dissipation-noise effect on the entanglement dynamics, while the sub-Ohmic and super-Ohmic environments induce much more severe noise. In particular, the memory of the system interacting with the environment contributes a strong decoherence effect to the entanglement dynamics in the super-Ohmic case.

PACS number(s): 03.65.Yz, 03.67.−a

I. INTRODUCTION

Quantum teleportation incorporating the classical communication theory with a unique characteristic of quantum mechanics, quantum entanglement, has received tremendous attention in the study of quantum communication in the past decade [1–3]. In quantum teleportation protocols, a necessary ingredient is the quantum channel, which is realized through an entangled quantum state of two systems separated between the sender and the receiver. Theoretically, both the discrete- (for example, two polarized photons, two-level atoms, or the spins of electrons, etc.) [4–9] and the continuous-variable (coherent and squeezed optical fields) [10,11] entangled states are equally useful for a quantum channel. Practically, compared with the discrete-variable entangled state, the continuous-variable entangled state may be more efficient because it has less decoherence [12–14]. Continuous-variable entangled states can be traced back to the original paper on quantum entanglement by Einstein, Podolsky, and Rosen [15], where entangled states of the common eigenstate of relative position and total momentum of two particles were proposed. Such ideal entangled states can actually be realized by a two-mode squeezed state of optical fields in the large limit of the squeezing parameter. In fact, the entangled two-mode optical squeezed state has been successfully produced via the nonlinear process of parametric down-conversion [16]. This triggered a variety of experiments [12–14] applying such an entangled state to quantum teleportation. The entangled two-mode optical squeezed state has been of key importance as an entangled resource for practical implementations of quantum-information protocols [3]. However, a realistic analysis of any quantum channel must take into account the noise effect from its environment. There has been an increasing interest in describing continuous-variable entanglement dynamics under noise [17–26].

The traditional approach to studying environment-induced noise effects treats the interaction between the quantum system and its environment perturbatively, which yields approximate equations of motion such as Redfield or master equations under the Born-Markov approximation [27–29]. Although this treatment has been widely employed in the field of quantum optics, where the characteristic time of the environmental correlation function is much shorter compared with that of the system investigated [29], its validity is experiencing more and more challenges in facing new experimental evidences [30]. Moreover, the Born-Markov approximation is in general invalid in dealing with most condensed-matter problems, for example, a quantum system hosted in a nanostructured environment [31–35], because large coupling constants and long correlation time scales of the environment both require a nonperturbative description. Therefore a nonperturbative description of the non-Markovian dynamics in open quantum systems has attracted much attention over recent years [36].

In fact, recently, non-Markovian processes have been extensively studied in the entanglement dynamics of two continuous-variable systems, such as two harmonic oscillators or two-mode electromagnetic fields, interacting with bosonic environments [22–26]. In [22], the non-Markovian entanglement dynamic of two-mode Gaussian states is studied based on the master equation derived perturbatively using the projection operator method up to the second order with respect to the system-reservoir coupling constant (which actually corresponds to the Born approximation). In [23] the dynamics of two harmonic oscillators interacting with two uncorrelated reservoirs was formulated based on the Hu-Paz-Zhang master equation of quantum Brownian motion [39] but the non-Markovian entanglement dynamics is analyzed up to the second order of the system-reservoir coupling constant with Ohmic reservoirs. More recently, an exact master equation for two coupled harmonic oscillators linearly interacting with a common reservoir has been derived using the Feynman-Vernon influence functional theory [37–39], where the decoherence and disentangled dynamics of a bipartite displaced Gaussian states is studied within the

Markovian approximation [24]. In a very recent paper [26], the non-Markovian master equation of two coupled harmonic oscillators interacting with either two independent reservoirs or a common reservoir was derived perturbatively up to the second order of the system-reservoir coupling constant (i.e., also in the Born approximation), and the entangled dynamics of two-mode Gaussian states was analyzed with Ohmic reservoirs as well. In our previous work [25], we have derived the exact master equation for two coupled cavity fields under the influence of vacuum fluctuation using the Feynman-Vernon influence functional theory in the coherent-state path integral formalism [40], and studied the decoherence dynamics of the continuous-variable quantum channel in terms of entangled two-mode Glauber coherent states with Ohmic spectral density.

In the present work, we shall explore the non-Markovian influence of the vacuum fluctuation on the continuous-variable quantum channel in terms of an entangled two-mode squeezed state with different spectral densities, i.e., the Ohmic, the sub-Ohmic, and the super-Ohmic cases. To study the non-Markovian entanglement dynamics of the squeezed-state quantum channel under the influence of the vacuum fluctuation, we model the system as two cavity fields coupling to a common bosonic environment at zero temperature. We then use the Feynman-Vernon influence functional theory in the coherent-state path integral formalism that we have provided in our previous work [25] to study nonperturbatively the noise effect on the entanglement dynamics of the squeezed states. As is well known, the Feynman-Vernon influence functional theory enables us to treat both of the back actions from the environment to the system and the system to the environment self-consistently. The dissipation and noise dynamics of the quantum channel, going beyond the Born-Markov approximation, is then governed by an effective action associated with the influence functional containing all the influences of the environment on the system.

Utilizing this nonperturbative treatment, the resulting exact master equation can be expressed in an operator form with time-dependent coefficients describing the full dynamics of the back action between the system and the environment. We thereby investigate the non-Markovian entanglement dynamics of the quantum channel under the influence of environments with different spectral densities, i.e., Ohmic, sub-Ohmic, and super-Ohmic densities. The influence of the environment induces a shifted frequency $\Omega(t)$ and a decay rate $\Gamma(t)$ in each cavity mode, as well as a shifted coupling strength $\Omega'(t)$ and a correlated decay rate $\Gamma'(t)$ between the two modes. The entanglement dynamics depends sensitively on the different shifted coupling strengths $\Omega'(t)$ (noise-induced entanglement oscillation) and the decay rates $\Gamma(t)$ and $\Gamma'(t)$ (dissipation-induced suppression of quantum entanglement) for different spectral densities. We find that the Ohmic environment shows a weak dissipation-noise effect, while the sub-Ohmic environment leads to fast decoherence in the entanglement dynamics. The super-Ohmic environment has the strongest memory effect, which heavily suppresses the entanglement of the squeezed-state quantum channel.

The paper is organized as follows. In Sec. II, we introduce the model describing the non-Markovian entanglement dynamics of the continuous-variable quantum channel in terms of an entangled squeezed state, and we shall also briefly review the master equation we derived in [25]. In Sec. III, we use logarithmic negativity as an entanglement measure of continuous-variable states to discuss the entanglement dynamics of the squeezed state. The numerical results of the entanglement dynamics are given in Sec. IV, where we also analyze in detail the influences of the environment with different spectral densities on the quantum channel. Finally, a brief summary is made in Sec. VI.

II. THE HAMILTONIAN AND THE EXACT NON-MARKOVIAN MASTER EQUATION

A. The model Hamiltonian

Our system consists of two coupled cavity fields subject to a common environment. The Hamiltonian of the total system is given by [29,41]

$$H = H_S + H_E + H_I, \tag{1}$$

where

$$H_S = \hbar\omega_1 a_1^\dagger a_1 + \hbar\omega_2 a_2^\dagger a_2 + \hbar\kappa(a_1^\dagger a_2 + a_2^\dagger a_1),$$

$$H_E = \sum_k \hbar\omega_k b_k^\dagger b_k,$$

$$H_I = \sum_{l,k} \hbar(g_{lk} a_l^\dagger b_k + g_{lk}^* a_l b_k^\dagger)$$

are the Hamiltonians of the two cavity fields, the environment, and their interaction, respectively. The operators a_l and $a_l^\dagger$ ($l=1,2$) are the corresponding annihilation and creation operators of the lth cavity field with frequency ω_l, and κ is a real coupling constant between the two cavity fields, which can be realized by a beam splitter. The environment is modeled, as usual, by a set of harmonic oscillators described by the annihilation and creation operators b_k and $b_k^\dagger$ ($k=1,2,\ldots$). The coupling constants between the cavity fields and the environment are given by g_{lk}. In the present work we shall consider the entangled squeezed state used in the quantum teleprotation of continuous-variable states [14] where the two cavity fields are identical, i.e., $\omega_1=\omega_2\equiv\omega_0$. We also assume that the dominant dissipation and noise effects are induced by the vacuum fluctuation, so that the environment is at zero temperature and the two cavity fields should interact homogeneously with the environment, namely, $g_{1k}=g_{2k}\equiv g_k$.

In order to investigate the decoherence effect in the entanglement dynamics induced by the environment, a specification of the spectral density $J(\omega)$ of the environment is required. The spectral density characterizing the coupling strength of the environment to the cavity fields with respect to its frequencies is defined by

$$J(\omega) = \sum_k |g_k|^2 \delta(\omega - \omega_k). \tag{2}$$

In the continuum limit the spectral density may have the form

$$J(\omega) = \eta\omega\left(\frac{\omega}{\omega_c}\right)^{n-1}\exp\left(-\frac{\omega}{\omega_c}\right), \tag{3}$$

where ω_c is a cutoff frequency, and η a dimensionless coupling constant. The environment is classified as Ohmic if $n = 1$, sub-Ohmic if $0 < n < 1$, and super-Ohmic if $n > 1$ [42].

B. The exact master equation

The exact master equation describing decoherence dynamics of the two cavity fields can be derived with the Feynman-Vernon influence functional method [38,43] in the coherent-state representation [40]. The detailed derivation can be found in [25], and we give only a few key steps here for completeness. Going from the quantum mechanical equation $i\hbar\partial\rho_{\text{tot}}(t)/\partial t = [H,\rho_{\text{tot}}(t)]$, the reduced density matrix fully describing the dynamics of the two cavity fields is obtained by integrating out completely the environmental degrees of freedom,

$$\rho(\bar{\boldsymbol{\alpha}}_f,\boldsymbol{\alpha}'_f;t)$$

$$= \int d\mu(\boldsymbol{\alpha}_i)d\mu(\boldsymbol{\alpha}'_i)J(\bar{\boldsymbol{\alpha}}_f,\boldsymbol{\alpha}'_f;t|\bar{\boldsymbol{\alpha}}_i,\boldsymbol{\alpha}'_i;0)\rho(\bar{\boldsymbol{\alpha}}_i,\boldsymbol{\alpha}'_i;0), \tag{4}$$

where the reduced density matrix is obtained from the total density matrix tracing over the environmental degrees of freedom, $\rho(\bar{\boldsymbol{\alpha}}_f,\boldsymbol{\alpha}'_f;t) = \int d\mu(\mathbf{z})\langle\alpha_f,\mathbf{z}|\rho_{\text{tot}}(t)|\alpha'_f,\mathbf{z}\rangle$, the complex variables $\boldsymbol{\alpha} = (\alpha_1,\alpha_2)$ and $\mathbf{z} = (z_1,z_2,\ldots)$ are the corresponding eigenvalues of the cavity-field operators $a_{1,2}$ and the environment operators b_k ($k = 1,2,\ldots$), acting on the bosonic coherent-state $|\boldsymbol{\alpha},J\rangle$, respectively, and $\bar{\boldsymbol{\alpha}}$ denotes the complex conjugate of $\boldsymbol{\alpha}$. The propagating function $J(\bar{\boldsymbol{\alpha}}_f,\boldsymbol{\alpha}'_f;t|\bar{\boldsymbol{\alpha}}_i,\boldsymbol{\alpha}'_i;0)$ has the form

$$J(\bar{\boldsymbol{\alpha}}_f,\boldsymbol{\alpha}'_f;t|\bar{\boldsymbol{\alpha}}_i,\boldsymbol{\alpha}'_i;0) = \int D^2\boldsymbol{\alpha}D^2\boldsymbol{\alpha}'\exp\left(\frac{i}{\hbar}(S_S[\bar{\boldsymbol{\alpha}},\boldsymbol{\alpha}]\right.$$

$$\left.- S_S^*[\bar{\boldsymbol{\alpha}},\boldsymbol{\alpha}'])\right)\mathcal{F}[\bar{\boldsymbol{\alpha}},\boldsymbol{\alpha},\bar{\boldsymbol{\alpha}},\boldsymbol{\alpha}'], \tag{5}$$

where $S_S[\bar{\boldsymbol{\alpha}},\boldsymbol{\alpha}]$ is the action of the two cavity fields,

$$S_S[\bar{\boldsymbol{\alpha}},\boldsymbol{\alpha}] = \hbar\sum_{l\neq l'}\left(-i\bar{\alpha}_{lf}\alpha_l(t) + \int_0^t d\tau[i\bar{\alpha}_l(\tau)\dot{\alpha}_l(\tau)\right.$$

$$\left.- \Delta_l\bar{\alpha}_l(\tau)\alpha_l(\tau) - \kappa\bar{\alpha}_l(\tau)\alpha_{l'}(\tau)]\right),$$

and $\mathcal{F}[\bar{\boldsymbol{\alpha}},\boldsymbol{\alpha},\bar{\boldsymbol{\alpha}}',\boldsymbol{\alpha}']$ is the Feynman-Vernon influence functional obtained after integrating out all the degrees of freedom of the environment,

$$\mathcal{F}[\bar{\boldsymbol{\alpha}},\boldsymbol{\alpha},\bar{\boldsymbol{\alpha}}',\boldsymbol{\alpha}'] = \exp\left[\int_0^t d\tau\int_0^\tau d\tau'\left(\sum_{l,m=1}^2(\bar{\alpha}'_l - \bar{\alpha}_l)(\tau)\right.\right.$$

$$\times\mu(\tau - \tau')\alpha_m(\tau') + (\alpha_l - \alpha'_l)(\tau)$$

$$\left.\left.\times\mu^*(\tau - \tau')\bar{\alpha}'_m(\tau')\right)\right].$$

The time-dependent function $\mu(\tau)$ is the dissipation-noise kernel characterizing the full influence of the environment on the two cavity fields,

$$\mu(\tau) = \sum_k e^{-i\omega_k(\tau)}|g_k|^2 = \int d\omega\, J(\omega)e^{-i\omega(\tau)}, \tag{6}$$

and is completely determined by the spectral density $J(\omega)$. We shall consider only the spectral density given by (3) in this paper.

As we see, all the effects of the environment on the system are incorporated into the influence functional, which effectively modifies the action of the cavity system. Since the resulting effective action is bilinear in terms of the cavity field variables $\boldsymbol{\alpha}$ and $\boldsymbol{\alpha}'$, the evaluation of the path integral over $\boldsymbol{\alpha}$ and $\boldsymbol{\alpha}'$ can be exactly executed with the saddle point method. This leads to the dissipation-noise equations ($l \neq l'$)

$$\dot{\alpha}_l + i(\omega_l\alpha_l + \kappa\alpha_{l'}) = -\int_0^\tau d\tau'\sum_{m=1}^2\mu(\tau - \tau')\alpha_m(\tau'),$$

$$\bar{\alpha}'_l - i(\omega_l\bar{\alpha}'_l + \kappa\bar{\alpha}'_{l'}) = -\int_0^\tau d\tau'\sum_{m=1}^2\mu^*(\tau - \tau')\bar{\alpha}'_m(\tau'), \tag{7}$$

obeying the boundary conditions $\alpha_l(0) = \alpha_{li}$ and $\bar{\alpha}'_l(0) = \bar{\alpha}'_{li}$. The integro-differential dissipation-noise equations render the reduced dynamics non-Markovian, with the memory of the system interacting with the environment registered in the dissipation-noise kernel $\mu(\tau - \tau')$. Introducing the new variables $u(t)$ and $v(t)$ by

$$\alpha_l(\tau) = \alpha_{li}u(\tau) - \alpha_{l'i}v(\tau),$$

$$\bar{\alpha}'_l(\tau) = \bar{\alpha}'_{li}\bar{u}(\tau) - \bar{\alpha}'_{l'i}\bar{v}(\tau), \quad l \neq l', \tag{8}$$

we obtain an explicit solution for the propagating function,

$$J(\bar{\boldsymbol{\alpha}}_f,\boldsymbol{\alpha}'_f;t|\bar{\boldsymbol{\alpha}}_i,\boldsymbol{\alpha}'_i;0) = \exp\left(\sum_{l=1}^2[u\bar{\alpha}_{lf}\alpha_{li} + \bar{u}\bar{\alpha}'_{li}\alpha'_{lf} - (\bar{u}u + \bar{v}v\right.$$

$$- 1)\bar{\alpha}'_{li}\alpha_{li}] - \sum_{l\neq l'}[v\bar{\alpha}_{lf}\alpha_{l'i} + \bar{v}\bar{\alpha}'_{li}\alpha'_{l'f}$$

$$\left.- (\bar{u}v + \bar{v}u)\bar{\alpha}'_{li}\alpha_{l'i}]\right). \tag{9}$$

The non-Markovian master equation can be deduced from (4) and (9). The result is [25]

$$\dot{\rho}(t) = -\frac{i}{\hbar}[H'(t),\rho(t)] + \Gamma(t)[2a_1\rho(t)a_1^\dagger - a_1^\dagger a_1\rho(t)$$

$$- \rho(t)a_1^\dagger a_1] + \Gamma(t)[2a_2\rho(t)a_2^\dagger - a_2^\dagger a_2\rho(t) - \rho(t)a_2^\dagger a_2]$$

$$+ \Gamma'(t)[2a_1\rho(t)a_2^\dagger - a_1^\dagger a_2\rho(t) - \rho(t)a_1^\dagger a_2] + \Gamma'(t)$$

$$\times[2a_2\rho(t)a_1^\dagger - a_2^\dagger a_1\rho(t) - \rho(t)a_2^\dagger a_1], \tag{10}$$

where

$$H'(t) = \hbar\Omega(t)(a_1^\dagger a_1 + a_2^\dagger a_2) + \hbar\Omega'(t)(a_1^\dagger a_2 + a_2^\dagger a_1),$$

with

$$\frac{u\dot{u} - v\dot{v}}{u^2 - v^2} \equiv -\Gamma(t) - \frac{i}{\hbar}\Omega(t), \quad \frac{v\dot{u} - u\dot{v}}{u^2 - v^2} \equiv -\Gamma'(t) - \frac{i}{\hbar}\Omega'(t). \tag{11}$$

This is the exact master equation for the dynamics of the two cavity fields, $\Omega(t)$ plays the role of a shifted time-dependent frequency for each cavity field, $\Omega'(t)$ accounts for a shifted time-dependent coherent coupling between the two cavity fields, $\Gamma(t)$ represents a time-dependent individual decay rate of each cavity field, and $\Gamma'(t)$ is a correlated decay rate between the two cavity fields. From Eq. (10), we can see that besides the spontaneous decay of the individual cavity field, the environment, even if only the vacuum fluctuation is concerned, also induces a coherent coupling and a correlated spontaneous decay between the two cavity fields. The non-Markovian character thus resides in these time-dependent coefficients in the master equation. We must emphasize that our derivation of the master equation, Eq. (10), is fully nonperturbative, which goes beyond the Born approximation [22,26] and involves all the back actions between the environment and the cavity fields.

III. ENTANGLEMENT MEASURE OF CONTINUOUS-VARIABLE QUANTUM CHANNELS AND ITS DYNAMICS

A. Logarithmic negativity as entanglement measure

In what follows, we shall analyze the effects of the different types of noise on the entanglement dynamics of the quantum channel in terms of an entangled two-mode squeezed state. The entangled two-mode squeezed state is defined as the vacuum state acted on by the two-mode squeezing operator

$$|\psi(0)\rangle = e^{r(a_1 a_2 - a_1^\dagger a_2^\dagger)}|00\rangle, \tag{12}$$

where r is the squeezing parameter. The state approaches the ideal Einstein-Podolsky-Rosen (EPR) state in the limit of infinite squeezing $(r \to \infty)$ [15]. After generating the entangled state given by Eq. (12), the two cavity fields are then propagated, respectively, to the two locations separated between the sender and the receiver. The quantum channel is thus established through the entangled two-mode squeezed state and is ready for teleporting unknown optical coherent states [11,14]. The traditional way to generate the entangled two-mode squeezed state is via the nonlinear optical process of parametric down-conversion [16]. Recently, a microwave cavity QED-based scheme to generate such states has also been proposed [44].

To investigate the entanglement dynamics of the quantum channel in terms of the two-mode squeezed state, a computable entanglement measure for such continuous-variable states must be defined first. Here we shall use the logarithmic negativity [45] to quantify the degree of entanglement in the quantum channel. The logarithmic negativity of a bipartite system was introduced originally as

$$E_N = \log_2 \sum_i |\lambda_i^-|, \tag{13}$$

where λ_i^- is the negative eigenvalue of ρ^{T_i}, and ρ^{T_i} is a partial transpose of the bipartite state ρ with respect to the degrees of freedom of the ith party. This measure is based on the Peres-Horodecki criterion [46,47] that a bipartite quantum state is separable if and only if its partially transposed state is still positive.

For the continuous-variable (Gaussian-type) bipartite state, its density matrix is characterized by the covariance matrix defined as the second moments of the quadrature vector $X = (x_1, p_1, x_2, p_2)$,

$$V_{ij} = \frac{\langle \Delta X_i \Delta X_j + \Delta X_j \Delta X_i \rangle}{2}, \tag{14}$$

where $\Delta X_i = X_i - \langle X_i \rangle$, and $x_i = (a_i + a_i^\dagger)/\sqrt{2}$, $p_i = (a_i - a_i^\dagger)/i\sqrt{2}$. The canonical commutation relations take the form as $[X_i, X_j] = iU_{ij}$, with $U = \begin{pmatrix} J & 0 \\ 0 & J \end{pmatrix}$ and $J = \begin{pmatrix} 0 & 1 \\ -1 & 0 \end{pmatrix}$ defining the symplectic structure of the system. The property of the covariance matrix V is fully determined by its symplectic spectrum $\nu = (\nu_1, \nu_2)$, with $\pm\nu_i$ ($\nu_i > 0$) the eigenvalues of the matrix: iUV. The uncertainty principle exerts a constraint on ν_i such that $\nu_i \geq \frac{1}{2}$ [49]. Thus the Peres-Horodecki criterion for the continuous-variable state can be rephrased as the state being separable if and only if the uncertainty principle $V + (i/2)U \geq 0$ is still obeyed by the covariance matrix under partial transposition with respect to the degrees of freedom of a specific subsystem [48]. In terms of phase space, the action of partial transposition amounts to a mirror reflection with respect to one of the canonical variables of the related subsystem. For instance, $\widetilde{V} = \Lambda V \Lambda$, and $\Lambda = diag(1, 1, 1, -1)$ is the partial transposition with respect to the second subsystem. If a Gaussian-type bipartite state is nonseparable, the covariance matrix $\widetilde{V}$ will violate the uncertainty principle and its symplectic spectrum $\widetilde{\nu} = (\widetilde{\nu}_1, \widetilde{\nu}_2)$ will fail to satisfy the constraint $\widetilde{\nu}_i \geq \frac{1}{2}$. The logarithmic negativity is then used to quantify this violation as [45]

$$E_N = \max\{0, -\log_2(2\widetilde{\nu}_{\min})\}, \tag{15}$$

where $\widetilde{\nu}_{\min}$ is the smaller one of the two symplectic eigenvalues $\widetilde{\nu}_i$. It is evident from Eq. (15) that, if $\widetilde{V}$ obeys the uncertainty principle, i.e., $\widetilde{\nu}_i \geq \frac{1}{2}$, then $E_N(\rho) = 0$, namely, the state is separable. Otherwise, it is entangled. Therefore, the symplectic eigenvalue $\widetilde{\nu}_{\min}$ encodes a qualitative feature of the entanglement for an arbitrary continuous-variable bipartite state.

B. The entanglement dynamics

With this entanglement measure at hand, we study now the entanglement dynamics of the squeezed-state quantum channel in our model. A straightforward way to obtain the time-dependent solution of the entangled squeezed state is by integrating the propagator function over the initial state of Eq. (4), where the initial state in coherent-state representation is given by

$$\rho(\bar{\boldsymbol{\alpha}}_i, \boldsymbol{\alpha}_i'; 0) = \frac{\exp[-\tanh r(\bar{\alpha}_{1i}\bar{\alpha}_{2i} + \alpha_{1i}'\alpha_{2i}')]}{\cosh^2 r}. \quad (16)$$

The solution of the reduced density matrix can be obtained exactly,

$$\rho(\bar{\boldsymbol{\alpha}}_f, \boldsymbol{\alpha}_f'; t) = b_0 \exp\left[\sum_{l\neq l'}\left(b_1\bar{\alpha}_{lf}^2 + b_2\alpha_{lf}'^2 + b_4\bar{\alpha}_{lf}\alpha_{lf}'\right.\right.$$
$$\left.\left. + b_5\bar{\alpha}_{lf}\alpha_{l'f}' + \frac{b_3}{2}\bar{\alpha}_{lf}\bar{\alpha}_{l'f} + \frac{b_6}{2}\alpha_{lf}'\alpha_{l'f}'\right)\right], \quad (17)$$

where the time-dependent parameters b_i $(i=0,\ldots,6)$ are given explicitly in the Appendix.

From the above solution, the covariance matrix V can be calculated analytically, and the logarithmic negativity $E_N(t)$ can also be obtained exactly from Eq. (15). It is easy to verify that the initial entanglement is $E_N(0)=2r/\ln 2$. While the asymptotical behavior of the entanglement (in the long-time limit) can be found from the solution

$$\rho(t \to \infty) = |\psi_{asy.}\rangle\langle\psi_{asy.}|,$$

$$|\psi_{asy.}\rangle = \sqrt{b_0'}e^{b_1'(a_1^\dagger - a_2^\dagger)^2}|00\rangle, \quad (18)$$

where $b_0' = b_0(t \to \infty) = 1/\cosh r$ and $b_1' = b_1(t \to \infty) = (\tanh re^{-2i(\omega_0-\kappa)t})/4$. This asymptotical solution results in

$$E_N(t \to \infty) = \frac{r}{\ln 2}, \quad (19)$$

namely, the final entanglement is only one-half of the initial value. Equation (19) indicates that the environment does decrease the entanglement of the quantum channel, as a dissipation-noise effect. This asymptotical result is also consistent with the Markovian limit at zero temperature in [17], since the non-Markovian dynamics must be asymptotically reduced to the Markovian limit [25].

It should be noted that the noise behavior of the quantum channel also depends on the structure of the initial two-mode squeezed state. This can be easily seen if we introduce the operators related to the center-of-mass and relative motional variables of the two cavity fields as $A^\dagger = (a_1^\dagger + a_2^\dagger)$ and $a^\dagger = (a_1^\dagger - a_2^\dagger)$, respectively. Then the initial state can be rewritten in terms of these two operators,

$$|\psi(0)\rangle = \frac{1}{\cosh r}e^{-[(\tanh r)/4](A^{\dagger 2}-a^{\dagger 2})}|00\rangle. \quad (20)$$

Since the two cavity fields interact homogeneously with the environment, namely, $g_{1k}=g_{2k}=g_k$, the interaction between the cavity fields and the environment only influences the dynamics of the center-of-mass variable; it has no effect on the relative motion of the two cavity fields (a similar discussion for two harmonic oscillators interacting with a common reservoir is given in [24]). In other words, the part of the squeezed state relating to the relative variable is immune to the environment, while that of the center of mass experiences
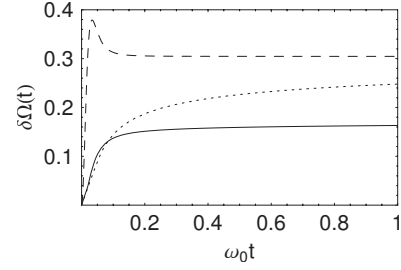

FIG. 1. Time dependence of the frequency shift $\delta\Omega(t)$ $[=\delta\Omega'(t)]$ induced by the environment with spectral density (3) of $n=1$ for the Ohmic (solid line), $n=3$ for the super-Ohmic (dashed line), and $n=1/2$ for the sub-Ohmic case (dotted line). The asymptotical value $\delta\Omega(t \to \infty)=\eta\omega_c$, $\sqrt{\pi}\eta\omega_c$, and $2\eta\omega_c$ for the Ohmic, super-Ohmic, and sub-Ohmic cases, respectively. The parameters in (3) are taken as $\eta=0.005$ and $\omega_c=30.0\omega_0$, while the coupling constant between the cavity fields and coupling constant $\kappa=0.5\omega_0$.

severe dissipation and noise from the environment. This results in the solution (18). One can verify that Eq. (18) is indeed a decoherence-free squeezed state [50], i.e., $|\psi_{DFS}\rangle \propto e^{x(a_1^\dagger - a_2^\dagger)^2}|00\rangle$. If such a state serves as the quantum channel, the quantum channel is free from the vacuum fluctuation, and the entanglement is preserved.

IV. NUMERICAL ANALYSIS OF THE NON-MARKOVIAN ENTANGLEMENT DYNAMICS

The full entanglement dynamics of the squeezed-state quantum channel is determined by the reduced density matrix obeying the master equation (10). To solve the master equation, we must find first the time-dependent coefficients contained in the master equation, the shifted frequency $\Omega(t)$ and the shifted coherent coupling $\Omega'(t)$, as well as the individual and correlated decay rates $\Gamma(t)$ and $\Gamma'(t)$. These coefficients are completely determined by the functions $u(t)$ and $v(t)$ as the solutions of the dissipation-noise equations (7) via (8). However, the dissipation-noise equations have to be solved numerically for the general environmental spectral density (3).

In Figs. 1 and 2, we plot the numerical results for the frequency shift $\delta\Omega(t) \equiv \omega_0 - \Omega(t)$ and decay rate $\Gamma(t)$ of the individual cavity field. We choose three different spectral densities: $n=1$, $1/2$, and 3 for the Ohmic, the sub-Ohmic, and the super-Ohmic spectral densities, respectively. Since the two cavity fields are considered to be identical ($\omega_1=\omega_2=\omega_0$) and interact homogeneously with the common environment ($g_{1k}=g_{2k}=g_k$), the environment-induced shifts of the field frequencies and the coherent coupling between the two cavity fields are equal, i.e., $\delta\Omega(t)=\delta\Omega'(t)$ where $\delta\Omega'(t) \equiv \kappa - \Omega'(t)$. The individual and correlated decay rates are also equal to each other, $\Gamma(t)=\Gamma'(t)$, for the same reason. From Figs. 1 and 2, we find that the dissipation-noise dynamics is characterized by two time scales: $\tau_1=\omega_c^{-1}$ (the shortest time scale of the environment) and $\tau_2=\omega_0^{-1}$ (the time scale of the cavity fields). When $t < \tau_1$, both coefficients $\delta\Omega(t)$ and $\Gamma(t)$ grow very quickly. After τ_1, they approach
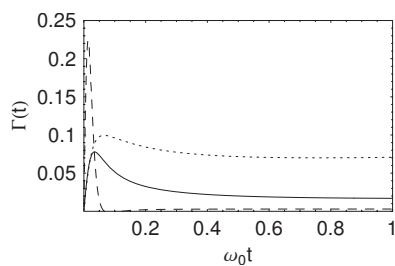
FIG. 2. Time dependence of the decay rate $\Gamma(t)$ $[=\Gamma'(t)]$ with $n=1$ for the Ohmic (solid line), $n=3$ for the super-Ohmic (dashed line), and $n=1/2$ for the sub-Ohmic (dotted line) environments. The input parameters in the numerical calculation are the same as in Fig. 1.

the corresponding asymptotical values gradually in the time scale of τ_2. We should point out that the asymptotic values of $\delta\Omega(t)$ and $\Gamma(t)$ in the Ohmic spectral density reproduce the Markovian limit, as we have shown in our previous work [25]). Compared with the super-Ohmic case, the sub-Ohmic dissipation shows a slower asymptotical tendency in the time scale τ_2. This is because, in the super-Ohmic case, the short-time correlation (the ultraviolet mode) is dominant, while in the sub-Ohmic case, the long-time correlation (the infrared mode) becomes important.

In fact, Fig. 2 also tells us that the decay rate grows very fast in the time scale τ_1 and develops a jolt [39]. This peak manifests the significant effect of the non-Markovian dynamics, especially for the super-Ohmic case. In the usual Born-Markovian approximation used in the literature [17,18,20,21], the back action of the environment on the system is completely ignored by the assumption of the response time of the environment being much smaller than the characteristic time (τ_2) of the system. The decay rate becomes then time independent. The time dependence of the decay rate in the exact master equation (10) contains the full memory effect of the system interacting with the environment, as a result of the non-Markovian dynamics. The non-Markovian entanglement dynamics of the quantum channel thus becomes transparent due to the presence of the time dependence of these coefficients in the time scale τ_1. This short-time correlation will influence strongly the later-time entanglement dynamics of the squeezed state.
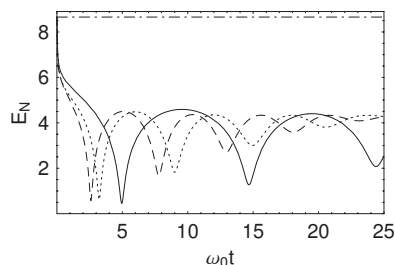

FIG. 3. Time evolution of the logarithmic negativity $E_N(t)$ without noise (dash-dotted line), and with the Ohmic (solid line), super-Ohmic (dashed line), and sub-Ohmic (dotted line) noise environments, in which the two cavity fields initially have no coupling to each other ($\kappa=0$). The other input parameters are still the same, and the squeezing parameter $r=3.0$.
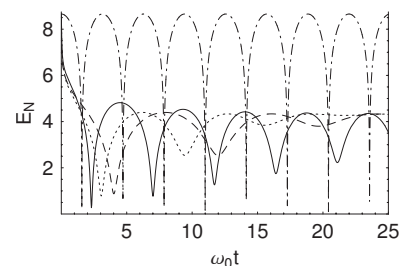

FIG. 4. Time evolution of the logarithmic negativity $E_N(t)$ without the noise effect (dash-dotted line), and with the Ohmic (solid line), super-Ohmic (dashed line), and sub-Ohmic (dotted line) noise environments. The input parameters are the same as in Figs. 3, except for $\kappa=0.5\omega_0$.

In Figs. 3 and 4, we plot the time evolution of the logarithmic negativity for the entanglement dynamics of the squeezed state. Figure 3 describes the case where the two cavity fields are initially decoupled ($\kappa=0$). As one would expect, in the absence of vacuum fluctuations the entanglement does not change in time. Figure 4 shows the coupling cavity fields ($\kappa=0.5$), where the entanglement undergoes a lossless periodic oscillation. When the vacuum fluctuation is taken into account, the entanglement dynamics is significantly changed as we see from Figs. 3 and 4. On one hand, the vacuum fluctuation induces entanglement oscillations (see Fig. 3) or shifts the oscillation frequencies of the entanglement oscillations (see Fig. 4) due to the effect of the shifted two-mode coupling $\delta\Omega'(t)$ (given in Fig. 1). We should mention that the entanglement oscillations have also been found for two uncoupled harmonic oscillators interacting with two independent reservoirs [23]. On the other hand, the amplitude of the entanglement oscillation is suppressed gradually and tends to its asymptotical value ($=r/\ln 2$) arising from the joint dissipation effects of the individual and correlated decay rates $\Gamma(t)$ and $\Gamma'(t)$. Furthermore, the dissipation will also erase the oscillation of entanglement arising from the coherent coupling between the two cavity fields. These decoherence effects are consistent with that obtained from the discrete qubit models [51]. It shows again that the asymptotic value of the entanglement reproduces the result in the Markovian limit [17].

One may also see from Figs. 3 and 4 that the entanglement dynamics behaves differently for three different spectral densities, as well as for the two coupled and uncoupled cavity fields. Comparing with the oscillation behaviors presented in Figs. 3 and 4, it shows that the order of the entanglement oscillations with three different spectral densities is reversed for the coupled and uncoupled cavity fields. This behavior comes mainly from the fact that the super-Ohmic environment induces the strongest entanglement oscillation; next is the sub-Ohmic case; while the Ohmic environment causes a relatively weak entanglement oscillation, as shown in Fig. 1. By the definition $\Omega'(t) \equiv \kappa - \delta\Omega'(t)$, it is easy to check that, for the uncoupled cavity fields, $\kappa=0$ so that $|\Omega'_{sup}(t)| > |\Omega'_{sub}(t)| > |\Omega'_{ohm}(t)|$. This leads to the frequencies of the entanglement oscillations $f_{sup} > f_{sub} > f_{ohm}$, as shown in Fig. 3. For the coupled cavity fields, $\kappa=0.5$ so that $|\Omega'_{sup}(t)| < |\Omega'_{sub}(t)| < |\Omega'_{ohm}(t)|$. This gives the frequency or-

dering $f_{sup} < f_{sub} < f_{ohm}$, as plotted in Fig. 4. This indicates that the non-Markovian induced entanglement oscillations can be quite different for the two coupled or uncoupled entangled cavity fields.

Meanwhile, the entanglement oscillation is sustained for the longest time in the Ohmic case, while the super- and sub-Ohmic environments cause severe decoherence. The sub-Ohmic (low-frequency) vacuum fluctuation induces a strong dissipative dynamics (the largest decay rate, as in Fig. 2), and therefore results in a fast decoherenc of the entanglement of the squeezed state, as expected. However, a remarkable result occurs in the super-Ohmic case where the entanglement and its oscillation are also strongly suppressed. In contrast to the sub-Ohmic case, the decay rate in the super-Ohmic case is almost negligible except for a sharp peak in the short-time scale τ_1, as shown in Fig. 2. We find that this short-time sharp peak induces a significant contribution to the entanglement decoherence in the quantum channel. This decoherence effect is a manifestation of the memory dynamics between the system and the environment. It is this non-Markovian dynamics that causes a rapid decoherence of the entanglement of the squeezed state in the super-Ohmic environment. We should note that, within the time scale $\tau_1 = \omega_c^{-1}$, the initial peak of the decay rates also exists in the Ohmic and sub-Ohmic cases although it is not as strong as in the super-Ohmic case. This initial "jolt" in the decay rates is indeed a general feature of the non-Markovian processes for the decoherence enhancement, as pointed out first by Hu *et al.* [39] in the study of quantum Brownian motion. The results we obtained in this work demonstrate that the non-Markovian dynamics also speed the decoherence of the entanglement in continuous-variable quantum channels.

V. SUMMARY

In the present work, we have studied the detrimental effects of the environment on the continuous-variable quantum channel in terms of the entangled two-mode squeezed state. Using the Feynman-Vernon influence functional theory in the coherent-state path integral representation, we derive the exact master equation for the two cavity fields under the influence of vacuum fluctuation [25] and then investigate the non-Markovian entanglement dynamics of the two-mode squeezed state quantum channel utilized in quantum teleportation [14] for three different spectral densities, the Ohmic, the sub-Ohmic, and the super-Ohmic non-Markovian environments. Very recently, a similar exact master equation has also been derived for two harmonic oscillators linearly coupled to a thermal bath where the entanglement dynamics is studied in the Markovian approximation [24].

We numerically study the non-Markovian entanglement dynamics of the quantum channel based on the exact master equation (10) for three different noise environments. Our numerical result indicates that the entanglement dynamics behaves different for the different environmental spectral densities which leads to significant distinctness in the time-dependent behavior of the dissipation-noise function, in particular, within the short time scale τ_1 of the environment. For Ohmic environment the system shows the longest quantum coherence because of the weak time-dependent dissipation of the entanglement dynamics of the squeezed state. In the sub-Ohmic case the squeezed state has a strong dissipation dynamics (corresponding to a large decay rate) induced mainly by the low-frequency noise of the environment, which results in fast decoherence for the entanglement dynamics of the squeezed state. The most significant evidence of the non-Markovian dynamics occurs in the super-Ohmic environment in which the strong non-Markovian process near the short time scale (τ_1) speeds the decoherence of the entanglement. These non-Markovian properties are indeed consistent with the non-Markovian phenomena explored in quantum Brownian motion [39].

We may also point out that for the squeezed-state quantum channel considered in this paper, both the asymptotical and the numerical solutions show that one-half of the initial entanglement carried by the squeezed state will be retained regardless of the spectral density of the environment. This is consistent with the solution in the Markovian limit [17]. This result depends only on the structure of the initial squeezed state as well as the property of the homogeneous coupling between the system and the environment. Thus the asymptotical state (18) is indeed a decoherence-free entangled squeezed state in our model, which may serve as a noiseless quantum channel for further applications in quantum communication. But it should be pointed out that, if the two cavity fields couple with two independent reservoirs, the above decoherence-free state no longer exists and the remaining entanglement will eventually be lost completely [23]. As our concentration is on the optical cavity fields, we have considered only the zero-temperature environment. A more general case, e.g., with the environment at a finite temperature, could hopefully be figured out a the similar approach to the derivation of Eq. (9). As robustness of the quantum channel is essential in view of decoherence, we hope that our consideration of non-Markovian entanglement dynamics in this paper provides useful information for experimental designs of quantum-information protocols.

APPENDIX: THE COEFFICIENTS OF $\rho(\overline{\alpha}_f, \alpha'_f; t)$ AND THEIR ASYMPTOTICAL BEHAVIORS

The explicit form of $\rho(\overline{\alpha}_f, \alpha'_f; t)$ is obtained from Eq. (4) by the evaluation of the integration. The final solution is given by Eq. (17) with the parameters

$$b_0 = \frac{1}{\cosh^2 r \sqrt{1 - 2\tanh^2 r(m^2 + n^2) + \tanh^4 r(m^2 - n^2)^2}},$$

$$b_1 = \frac{e\tanh^4 r[(un + vm)^2 + (um + wn)^2] + c\tanh^3 r(un + vm)(um + vn)}{1 - 2\tanh^2 r(m^2 + n^2) + \tanh^4 r(m^2 - n^2)^2} + \tanh r uv,$$

$$b_2 = \frac{e\tanh^2 r(\bar{u}^2 + \bar{v}^2) + c\tanh r\bar{u}\bar{v}}{1 - 2\tanh^2 r(m^2 + n^2) + \tanh^4 r(m^2 - n^2)^2},$$

$$b_3 = \frac{e[-4\tanh^4 r(un + vm)(um + vn)] + c\{-\tanh^3 r[(un + vm)^2 + (um + vn)^2]\}}{1 - 2\tanh^2 r(m^2 + n^2) + \tanh^4 r(m^2 - n^2)^2} - \tanh r(u^2 + v^2),$$

$$b_4 = \frac{e\{-2\tanh^3 r[\bar{u}(un + vm) + \bar{v}(um + vn)]\} + c\{-\tanh^2 r[\bar{u}(um + vn) + \bar{v}(un + vm)]\}}{1 - 2\tanh^2 r(m^2 + n^2) + \tanh^4 r(m^2 - n^2)^2},$$

$$b_5 = \frac{e\{2\tanh^3 r[\bar{u}(um + vn) + \bar{v}(un + vm)]\} + c\{\tanh^2 r[\bar{u}(un + vm) + \bar{v}(um + vn)]\}}{1 - 2\tanh^2 r(m^2 + n^2) + \tanh^4 r(m^2 - n^2)^2},$$

$$b_6 = \frac{e(-4\tanh^2 r\bar{u}\bar{v}) + c[-\tanh r(\bar{u}^2 + \bar{v}^2)]}{1 - 2\tanh^2 r(m^2 + n^2) + \tanh^4 r(m^2 - n^2)^2},$$

where $c = 1 - \tanh^2 r(m^2 + n^2)$, $e = \tanh r mn$, $m = \bar{u}u + \bar{v}v - 1$, and $n = \bar{u}v + \bar{v}u$. In the long time limit, $u(t \to \infty) = v(t \to \infty) = e^{-i(\omega_0 - \kappa)t}/2$. Then

$$b_0(t \to \infty) = \frac{1}{\cosh r}, \quad b_4(t \to \infty) = b_5(t \to \infty) = 0,$$

$$b_1(t \to \infty) = b_2^*(t \to \infty) = \frac{-b_3(t \to \infty)}{2} = \frac{-b_6^*(t \to \infty)}{2}$$

$$= \frac{\tanh r e^{-2i(\omega_0 - \kappa)t}}{4}.$$

[1] C. H. Bennett, G. Brassard, C. Crepeau, R. Jozsa, A. Peres, and W. K. Wootters, Phys. Rev. Lett. **70**, 1895 (1993).

[2] M. A. Nielsen and I. L. Chuang, *Quantum Computation and Quantum Information* (Cambridge University Press, Cambridge, U. K., 2000).

[3] S. L. Braunstein and P. van Loock, Rev. Mod. Phys. **77**, 513 (2005), and references therein.

[4] D. Bouwmeester, J.-W. Pan, K. Matter, M. Eibl, H. Weinfurter, and A. Zeilinger, Nature (London) **390**, 575 (1997).

[5] E. Hagley, X. Maitre, G. Nogues, C. Wunderlich, M. Brune, J. M. Raimond, and S. Haroche, Phys. Rev. Lett. **79**, 1 (1997).

[6] M. A. Rowe, D. Kielpinski, V. Meyer, C. A. Sackett, W. M. Itano, C. Monroe, and D. J. Wineland, Nature (London) **409**, 791 (2001).

[7] W. D. Oliver, F. Yamaguchi, and Y. Yamamoto, Phys. Rev. Lett. **88**, 037901 (2002).

[8] T. Yamamoto, M. Koashi, S. K. Özdemir, and N. Imoto, Nature (London) **421**, 343 (2003).

[9] M. Riebe, H. Häffner, C. F. Roos, W. Hänsel, M. Ruth, J. Benhelm, G. P. T. Lancaster, T. W. Körber, C. Becher, F. Schmidt-Kaler, D. F. V. James, and R. Blatt, Nature (London) **429**, 734 (2004).

[10] L. Vaidman, Phys. Rev. A **49**, 1473 (1994).

[11] S. L. Braunstein and H. J. Kimble, Phys. Rev. Lett. **80**, 869 (1998).

[12] W. P. Bowen, N. Treps, B. C. Buchler, R. Schnabel, T. C. Ralph, Hans.-A. Bachor, T. Symul, and P. K. Lam, Phys. Rev. A **67**, 032302 (2003).

[13] T. C. Zhang, K. W. Goh, C. W. Chou, P. Lodahl, and H. J. Kimble, Phys. Rev. A **67**, 033802 (2003).

[14] A. Furusawa, J. L. Sorensen, S. L. Braunstein, C. A. Fuchs, H. J. Kimble, and E. S. Polzik, Science **282**, 706 (1998).

[15] A. Einstein, B. Podolsky, and N. Rosen, Phys. Rev. **47**, 777 (1935).

[16] Z. Y. Ou, S. F. Pereira, H. J. Kimble, and K. C. Peng, Phys. Rev. Lett. **68**, 3663 (1992).

[17] J. S. Prauzner-Bechcicki, J. Phys. A **37**, L173 (2004).

[18] J.-H. An, S.-J. Wang, and H.-G. Luo, J. Phys. A **38**, 3579 (2005).

[19] H. McAneney *et al.*, J. Mod. Opt. **52**, 935 (2005).

[20] R. Rossi, Jr., A. R. Bosco de Magalhães, and M. C. Nemes, Physica A **365**, 402 (2006).

[21] G. Adesso, A. Serafini, and F. Illuminati, Phys. Rev. A **73**, 032345 (2006).

[22] M. Ban, Phys. Lett. A **359**, 402 (2006); M. Ban, J. Phys. A **39**, 1927 (2006).

[23] S. Maniscalco, S. Olivares, and M. G. A. Paris, Phys. Rev. A **75**, 062119 (2007).

[24] C. H. Chou, T. Yu, and B. L. Hu, e-print arXiv:quant-ph/0703088.

[25] J.-H. An, M. Feng, and W.-M. Zhang, e-print arXiv:0705.2472.

[26] K. L. Liu and H. S. Goan, Phys. Rev. A **76**, 022312 (2007).

[27] A. G. Redfield, Adv. Magn. Reson. **1**, 1 (1965).

[28] G. Lindblad, Commun. Math. Phys. **48**, 119 (1976).

[29] H. J. Carmichael, *An Open Systems Approach to Quantum Optics*, Lecture Notes in Physics Vol. m18 (Springer-Verlag, Berlin, 1993).

[30] F. Dublin, D. Rotter, M. Mukherjee, C. Russo, J. Eschner, and R. Blatt, Phys. Rev. Lett. **98**, 183003 (2007).

[31] S. John and T. Quang, Phys. Rev. Lett. **74**, 3419 (1994).

[32] G. Aquino, L. Palatella, and P. Grigolini, Phys. Rev. Lett. **93**, 050601 (2004).

[33] A. A. Budini, Phys. Rev. A **73**, 061802(R) (2006).

[34] M. T. Lee and M. W. Zhang, Phys. Rev. B **74**, 085325 (2006).

[35] G. Falci, A. D'Arrigo, A. Mastellone, and E. Paladino, Phys. Rev. Lett. **94**, 167002 (2005).

[36] H.-P. Breuer and F. Petruccione, *The Theory of Open Quantum Systems*, (Oxford University Press, Oxford, 2002).

[37] R. P. Feynman and F. L. Vernon, Ann. Phys. (N.Y.) **24**, 118

[38] A. O. Caldeira and A. J. Leggett, Physica A **121**, 587 (1983).

[39] B. L. Hu, J. P. Paz, and Y. Zhang, Phys. Rev. D **45**, 2843 (1992).

[40] W. M. Zhang, D. H. Feng, and R. Gilmore, Rev. Mod. Phys. **62**, 867 (1990).

[41] G. Hackenbroich, C. Viviescas, and F. Haake, Phys. Rev. A **68**, 063805 (2003).

[42] A. J. Leggett, S. Chakravarty, A. T. Dorsey, M. P. A. Fisher, A. Garg, and W. Zwerger, Rev. Mod. Phys. **59**, 1 (1987).

[43] C. Anastopoulos and B. L. Hu, Phys. Rev. A **62**, 033821 (2000).

[44] S. Pielawa, G. Morigi, D. Vitali, and L. Davidovich, Phys. Rev. Lett. **98**, 240401 (2007).

[45] G. Vidal and R. F. Werner, Phys. Rev. A **65**, 032314 (2002).

[46] A. Peres, Phys. Rev. Lett. **77**, 1413 (1996).

[47] M. Horodecki, P. Horodecki, and R. Horodecki, Phys. Lett. A **223**, 1 (1996).

[48] R. Simon, Phys. Rev. Lett. **84**, 2726 (2000).

[49] G. Adesso and F. Illuminati, Phys. Rev. A **72**, 032334 (2005).

[50] D. A. Lidar, I. L. Chuang, and K. B. Whaley, Phys. Rev. Lett. **81**, 2594 (1998).

[51] J.-H. An, S.-J. Wang, and H.-G. Luo, Physica A **382**, 753 (2007).